ARTICLE

Divergent regulation of hepatic glucose and lipid metabolism by phosphoinositide 3-kinase via Akt and PKCλ/ζ

Cullen M. Taniguchi,[1] Tatsuya Kondo,[2] Mini Sajan,[3] Ji Luo,[4,5] Roderick Bronson,[6] Tomoichiro Asano,[7] Robert Farese,[3] Lewis C. Cantley,[4,5] and C. Ronald Kahn[1,*]

[1] Cellular and Molecular Physiology, Joslin Diabetes Center, Harvard Medical School, Boston, Massachusetts, 02215
[2] Department of Metabolic Medicine, Graduate School of Medical Sciences, Kumamoto University, Kumamoto, Japan
[3] University of South Florida, College of Medicine, Tampa, Florida 33612
[4] Department of Systems Biology, Harvard Medical School, Boston, Massachusetts, 02215
[5] Division of Signal Transduction, Beth Israel Deaconess Medical Center, Boston, Massachusetts 02115
[6] Department of Pathology, Harvard Medical School, Boston, Massachusetts, 02215
[7] Third Department of Internal Medicine, Faculty of Medicine, University of Tokyo, Tokyo 113, Japan
*Correspondence: c.ronald.kahn@joslin.harvard.edu

Summary

Although the class I_A phosphoinositide 3-kinase (PI3K) pathway is central to the metabolic actions of insulin, its mechanism of action is not well understood. To identify the role of the PI3K pathway in insulin regulation of hepatic function, we ablated the expression of both major regulatory subunits of PI3K by crossing mice lacking *Pik3r1* in liver with *Pik3r2* null mice, creating liver-specific double knockout mice (L-p85DKO). L-p85DKO mice failed to activate PI3K or generate PIP_3 upon insulin stimulation or activate its two major effectors, Akt and PKCλ/ξ. Decreased Akt activation resulted in increased gluconeogenic gene expression, impaired glucose tolerance, and hyperinsulinemia, while the defective activation of PKCλ/ξ by insulin was associated with hypolipidemia and decreased transcription of SREBP-1c. These data indicate that the PI3K pathway is critical for insulin's actions in the liver in vivo, and that differential regulation by Akt and PKCλ/ξ differentially defines specific actions of insulin and PI3K on hepatic glucose and lipid metabolism.

Introduction

Class I_A phosphoinositide 3-kinase (PI3K) is a critical mediator of insulin action in the liver (Taniguchi et al., 2006). Following insulin stimulation of its receptor, PI3K generates the second messenger phosphatidylinositol(3,4,5)-trisphosphate (PIP_3), which then activates several downstream targets such as Akt and atypical forms of protein kinase C (PKC λ/ζ) via their colocalization with PDK1. The PI3K-dependent activation of Akt defines many aspects of the insulin-mediated regulation of hepatic glucose metabolism. Akt suppresses gluconeogenesis and activates glycogen synthesis via its phosphorylation of FoxO1 (Zhang et al., 2002) and GSK3β (Cross et al., 1995), respectively. The PI3K/Akt axis also regulates cell growth via the phosphorylation and inhibition of hamartin and tuberin (TSC1 and TSC2) (Potter et al., 2002), which effectively activates the mTOR pathway resulting in phosphorylation of p70S6kinase and 4EBP1and stimulation of protein synthesis and cell growth (Harris and Lawrence, 2003).

Insulin also promotes hepatic lipogenesis through several mechanisms, the most prominent of which is upregulation of sterol regulatory element binding protein-1c (SREBP-1c), a transcription factor that potently activates the lipogenic program (Shimomura et al., 1999). The components of the PI3K pathway that are responsible for this increase in SREBP-1c expression are not well understood. Indeed, while Akt has potent effects on glucose metabolism, it exhibits only modest effects on lipogenesis and SREBP-1c mRNA levels both in vitro (Fleischmann and Iynedjian, 2000) and in vivo (Ono et al., 2003). Moreover, much of Akt's lipogenic effect may occur independently of SREBP (Ono et al., 2003). Recently, the atypical PKC isoforms λ and ζ that are activated by PI3K have been shown to be required for insulin-dependent increases in the expression of SREBP-1c (Farese et al., 2005). Thus, a liver-specific knockout of PKCλ leads to a marked decrease in SREBP-1c expression, with little effect on the expression of gluconeogenic genes, such as phosphoenolpyruvate carboxykinase (PEPCK) and glucose 6-phosphatase (G6Pase), suggesting that the atypical PKCs may positively regulate SREBP-1c expression in vivo (Matsumoto et al., 2003).

The dissection of the multiple functions of PI3K in vivo by genetic deletion has been difficult to achieve. Mammalian PI3K is a heterodimer that consists of an SH2-containing regulatory subunit (p85) and a catalytic subunit (p110), with both subunits expressed in multiple isoforms. There are eight isoforms of the regulatory subunit encoded by three different genes, *Pik3r1*, *Pik3r2*, and *Pik3r3*. In most cells, the gene products of *Pik3r1* constitute 65%–75% of the intracellular pool of regulatory subunits in the form of p85α and its two shorter isoforms p55α and p50α (Ueki et al., 2000), while *Pik3r2* accounts for 20%–30% of the regulatory subunits in the form of p85β (Ueki et al., 2003). The catalytic subunit of class I_A PI3K is also represented by three different isoforms—p110α, p110β, and p110δ—each of which is produced from a distinct gene (reviewed in Shepherd et al., 1998).

The complex roles of the PI3K subunits in embryonic development and metabolic homeostasis have confounded conventional

knockout studies of both the regulatory and catalytic subunits of PI3K. For instance, global knockouts of the p110α or p110β catalytic subunits cause early embryonic lethality (Bi et al., 2002; Bi et al., 1999), and the whole-body knockout of *Pik3r1* results in perinatal lethality (Fruman et al., 2000).

To study the effect of the in vivo loss of the PI3K pathway on hepatic glucose and lipid homeostasis and to circumvent the lethality encountered in various global knockouts of PI3K subunits, we have created mice which lack all PI3K regulatory subunits in liver (L-p85DKO) by crossing mice in which the *Pik3r1* gene (producing p85α, p55α, and p50α) is specifically inactivated in the liver (L-αKO mice) with *Pik3r2* knockout mice, which lack the other major p85 isoform, p85β, in all tissues. We find that deletion of both *Pik3r1* and *Pik3r2* in the liver completely ablates PI3K activity and the accumulation of PIP_3 resulting in a 90% decrease in Akt and PKCλ/ζ activation. By reconstitution experiments, we show that the loss of Akt activity in the L-p85DKO animals is linked to the defects in glucose homeostasis such as glucose intolerance and increased expression of gluconeogenic genes, while decreased PKCλ/ζ activity is associated with lower mRNA levels of SREBP-1c and hypolipidemia. These data suggest that the insulin/PI3K pathway regulates hepatic glucose and lipid homeostasis via distinct mediators, with Akt playing a more important role in the former and PKCλ/ζ activating the latter.

Results

L-p85DKO mice have significant defects in insulin-stimulated PIP_3 generation

Mice lacking *Pik3r1* and *Pik3r2* in liver were generated by crossing mice that were both homozygous for a floxed allele of *Pik3r1* (Luo et al., 2005) and heterozygous for the albumin-Cre transgene (Postic and Magnuson, 2000) with mice homozygous for both the *Pik3r1* floxed allele and the *Pik3r2* null allele (Ueki et al., 2002). Thus, these matings produced mice deleted of *Pik3r1* specifically in liver on a global p85β knockout background, i.e., a double knockout of *Pik3r1* and *Pik3r2* in liver (L-p85DKO). This breeding strategy (see Experimental Procedures) also generated four other study groups: *Pik3r1* homozygous floxed controls (FLOX), *Pik3r1* homozygous floxed mice that also lack *Pik3r2* (βKO), as well as mice with *Pik3r1* ablated only in liver either on a wild-type (wt) background (L-αKO) or on a *Pik3r2* heterozygous background (L-αKOβH). Western blotting with a pan-p85 antibody directed against the common C terminus of the regulatory subunits revealed an ~90% decrease of hepatic p85α and p50α expression in mice with a deletion of *Pik3r1* in liver, which is consistent with the amount of protein derived from hepatocytes (Figure 1A and Fruman et al., 2000). Since the pan-p85α antibody only weakly detects p85β and there are no good existing antibodies for p85β Western blotting, we confirmed the deletion of p85β by quantitative RT-PCR. Indeed, mice that were homozygous for a *Pik3r2* null allele exhibited no detectable levels of p85β mRNA after 40 cycles of quantitative RT-PCR, while mice heterozygous for *Pik3r2* displayed a 30% decrease of p85β mRNA (Figure 1B).

The genetic ablation of the regulatory subunits also decreased total hepatic PI3K activity to levels commensurate with p85 expression. Thus, when total PI3K activity was measured from phosphotyrosine (pTyr) immunoprecipitates of liver lysates, βKO animals that lack only 20% of total regulatory subunits exhibited no differences from FLOX controls. More severe disruptions of p85 expression, as in the L-αKO (L-*Pik3r1*$^{-/-}$, *Pik3r2*$^{+/+}$) or the L-αKOβH (L-*Pik3r1*$^{-/-}$, *Pik3r2*$^{+/-}$) mice, caused a 50% and 70% reduction in pTyr-associated PI3K activity, respectively (Figure 1C). As expected, when all four alleles of the regulatory subunits were deleted (L-*Pik3r1*$^{-/-}$, *Pik3r2*$^{-/-}$; L-p85DKO), insulin failed to stimulate PI3K activity above basal levels. In general, IRS-1- and IRS-2-associated PI3K activity reflected total PI3K activity, except that the loss of one or both alleles of *Pik3r2* resulted in increased IRS-2 activity, as previously noted (Ueki et al., 2002).

Germline knockouts of the regulatory subunit of PI3K have been complicated by discrepancies between PI3K activity and PIP_3 levels due to various compensatory effects (Terauchi et al., 1999). To determine levels of the second messenger PIP_3 in these knockout animals, we utilized an in situ immunofluorescence technique that allowed us to semiquantitatively measure PIP_3 levels in hepatocytes with an anti-PIP_3 antibody (Figure 1D; Kitamura et al., 2004). Surprisingly, PIP_3 levels in βKO and L-αKO mice were not statistically different from control FLOX mice, despite a 50% decrease in total PI3K activity in the latter (Figure 1C). More stringent deletions of regulatory subunits did produce statistically significant decreases in PIP_3 levels. L-αKOβH mice showed a 50% impairment of PIP_3 generation, while insulin-stimulated PIP_3 production in L-p85DKO mice was barely above basal levels. Thus, genetic ablation of the major regulatory subunit isoforms encoded by *Pik3r1* and *Pik3r2* can disrupt PI3K activity and function but only after severe deletions of at least three of the four major alleles encoding regulatory subunits.

Akt signaling is significantly impaired in L-p85DKO mice

The generation of PIP_3 by PI3K ultimately activates Akt, atypical PKCs, and other PH domain-containing proteins. As expected, L-p85DKO mice showed a 90% decrease in Akt activation, as measured by phosphorylation of serine 473 in Akt (Figure 2A). This correlated with impaired phosphorylation/activation of downstream Akt targets, including FoxO1 and GSK3β (Figure 2A). The phosphorylation of TSC2 was also significantly impaired (Figure 2B). Since TSC2 controls cell growth and protein synthesis via the mTOR/p70S6K pathway, we determined whether the loss of PI3K activity also disrupted mTOR signaling by measuring S6 phosphorylation since phosphorylation of ribosomal S6 is one of the ultimate downstream results of mTOR activation. As expected, insulin stimulation of S6 ribosomal protein phosphorylation exhibited a marked decrease in liver of L-αKOβH mice and was absent in L-p85DKO mice (Figure 2B).

Recent evidence has demonstrated that the different Akt isoforms may have unique roles in metabolic homeostasis (Jiang et al., 2003), with Akt2 playing a particularly dominant role in hepatic metabolism (Cho et al., 2001). To determine if the Akt isoforms were differentially affected by the deletion of p85, we measured the kinase activity of Akt1 (Figure 2C) and Akt2 (Figure 2D) using isoform-specific antibodies (Sakamoto et al., 2002). The kinase activities of both Akt1 and Akt2 paralleled Ser473 phosphorylation of Akt, with activity remaining normal unless all four alleles of p85 were deleted (Figures 2C and 2D). These data suggest that Akt is exquisitely sensitive to PIP_3 levels, and that even with a 50% decrease in PIP_3 generation, there is sufficient PIP_3 to promote the full activation of all Akt isoforms.

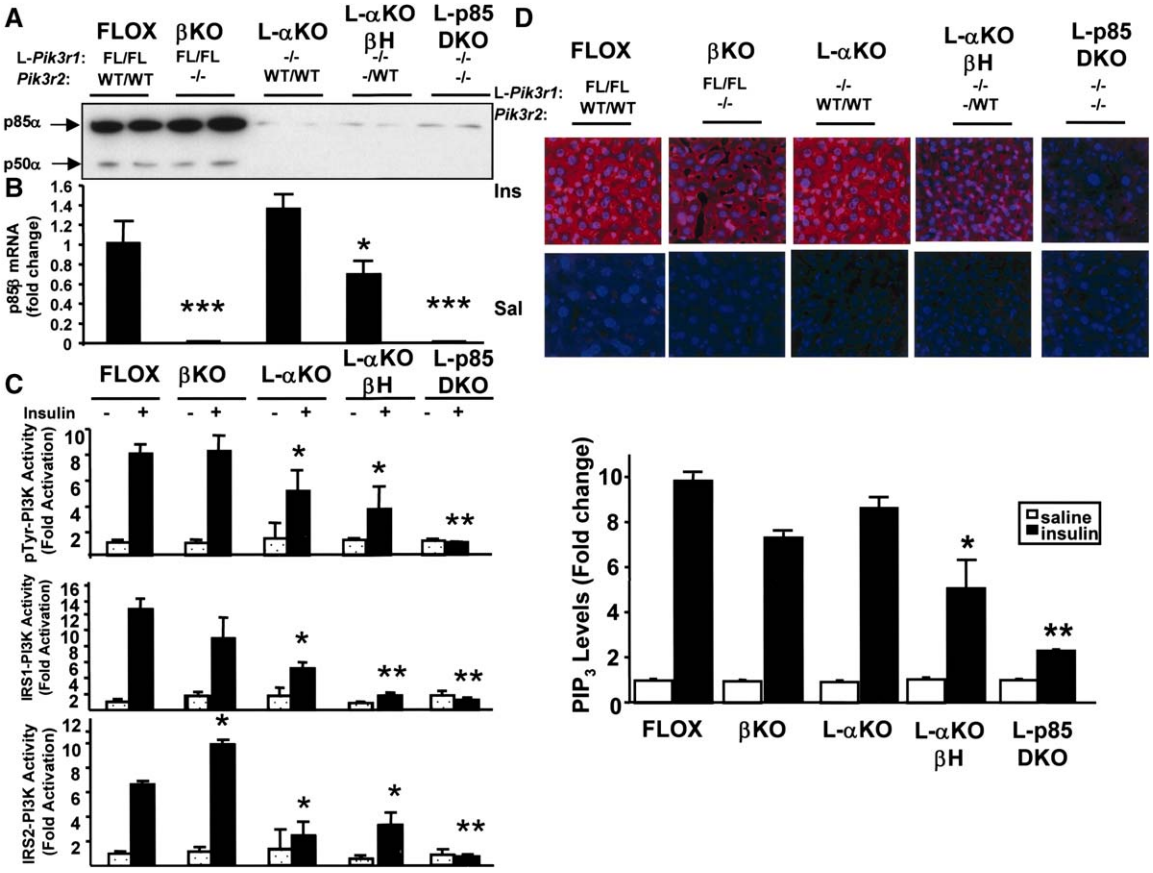

Figure 1. L-p85DKO mice have defective insulin-stimulated PI3K activity in liver

A) Immunoblot with a pan-p85α from liver lysates of mice of the indicated genotypes.

B) Quantitative RT-PCR analysis of p85β message levels. Bars represent means ± SEM, n = 6–8, *p < 0.05 compared to FLOX.

C) PI3K activity in pTyr, IRS-1, and IRS-2 immunoprecipitates. Bars represent means ± SEM, n = 4, *p < 0.05 compared to insulin stimulated FLOX.

D) (Top) Immunofluorescent staining with a primary anti-PIP_3 antibody (IgM) and an anti-mouse secondary antibody conjugated to Alexafluor Red. The sections were counterstained with DAPI. (Bottom) Quantification of the immunofluorescence from PIP_3 staining. Four representative slides were chosen from each mouse and the fluorescence intensity of 16 fields per slide was measured and analyzed with VH-H1A5 Analyzer software (KEYENCE, Osaka, Japan). Bars represent means ± SEM, *p < 0.05 compared to insulin-stimulated FLOX. **p < 0.01 and ***p < 0.0001.

L-p85DKO mice have severe defects in glucose homeostasis

The loss of the insulin stimulated activation of PI3K and Akt in the liver of L-p85DKO mice and led to significant defects in whole-body glucose homeostasis. Compared to FLOX controls, L-p85DKO mice exhibited mild to moderate hyperglycemia in both the fasted and fed states (Figures 3A and 3C). Furthermore, these blood glucose levels occurred in the fast of significant hyperinsulinemia, with insulin levels increased by 4-fold over control animals in L-p85DKO mice in both the fasted and fed states (Figures 3B and 3D). Interestingly, L-αKO mice exhibited improved glucose and insulin levels compared to controls, consistent with previous observations in mice lacking p85α (Fruman et al., 2000; Terauchi et al., 1999).

In addition, L-p85DKO mice exhibited insulin resistance and glucose intolerance. Following an intraperitoneal insulin injection (Figure 3E), mice lacking all hepatic PI3K regulatory subunits in liver showed a significant decrease in insulin sensitivity compared to FLOX controls, as determined by the area under the curve for fall in glucose levels (Figure 3F). Interestingly, L-p85DKO mice exhibit whole-body insulin resistance despite the fact that tissues other than the liver are only homozygous null for p85β, a defect that has previously been shown to improve insulin sensitivity (Ueki et al., 2002). L-p85DKO also exhibited markedly abnormal glucose tolerance tests consistent with diabetes (Figure 3G). For the L-p85DKO mice, the area under the curve was almost three times that of control mice (Figure 3H), whereas L-αKO mice exhibited improved glucose tolerance compared to FLOX controls (Figures 3G and 3H). Thus, while a partial deletion of the regulatory subunits may improve glucose homeostasis, loss of all PI3K regulatory subunits in liver results in diabetes.

The loss of hepatic PI3K/Akt activity leads to increased gluconeogenesis

One of the hallmarks of diabetes is increased hepatic glucose output due to failure of insulin to inhibit hepatic gluconeogenesis. Since L-p85DKO mice cannot activate Akt and thus phosphorylate and inactivate FoxO1, a key regulator of gluconeogenic gene expression, we posited that the gluconeogenic gene cassette should be dysregulated. Indeed, the mRNA levels of critical regulators of gluconeogenesis: PEPCK (*Pck1*), fructose 1,6-bisphosphatase (*Fbp1*), and glucose-6-phosphatase

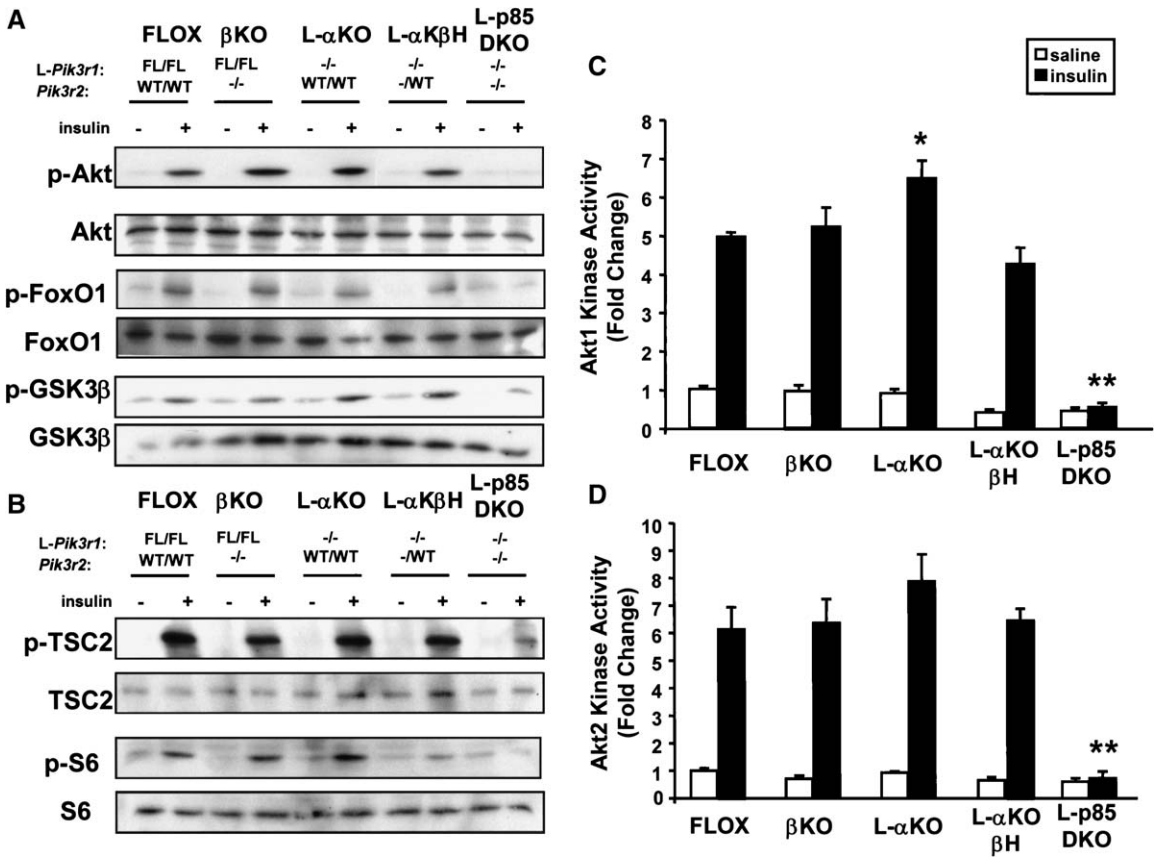

Figure 2. Loss of Hepatic PI3K Activity Leads to Defects in the Akt signaling

A) Liver lysates from insulin-stimulated mice of the indicated genotype were blotted with antibodies against phospho-Akt (Ser473), phospho-FoxO1 (Ser256), phospho-GSK3β (Ser9). The blots were then stripped and reprobed with antibodies to measure total protein levels.

B) Westerns against phospho-TSC2 (Thr1462) and phospho-S6 proteins (Ser240/244). The blots were then stripped and reprobed with antibodies to measure total protein levels. The Western blots in this figure are representative of at least three independent experiments.

C) Akt1 and (**D**) Akt2 kinase assays. (Bars represent ± SEM, n = 6, *$p < 0.05$, **$p < 0.001$, compared to FLOX + insulin).

(*G6pc*) in the L-p85DKO mice were increased 1.5- to 2.2-fold compared to controls (Figure 4A).

To determine whether this altered pattern of hepatic gene expression resulted in a functional defect, we subjected L-p85DKO mice and littermate FLOX and βKO controls to a pyruvate challenge. In fasting mice, pyruvate is shuttled through the gluconeogenic pathway in the liver and ultimately converted to glucose. Thus, by measuring blood glucose after a peritoneal injection of a pyruvate bolus, we are afforded a physiologic readout of the relative activity of the enzymes of the gluconeogenic pathway. Following an injection of pyruvate, L-p85DKO mice produced significantly more glucose than FLOX and βKO controls (Figure 4B), which indicate that the defects in glucose homeostasis in L-p85DKO mice may stem from the inappropriate gluconeogenesis in the liver due to a failure of insulin to activate PI3K and Akt.

L-p85DKO mice exhibit altered lipid metabolism

To better understand how the PI3K pathway affects lipid homeostasis, we measured serum levels of triglycerides, cholesterol, and free fatty acids (Figures 5A–5C). L-p85DKO mice showed a 46% reduction in serum triglycerides, a 38% reduction in total serum cholesterol, and a 35% reduction in free fatty acids compared to FLOX controls, which were all statistically significant. The other study groups were not statistically different from controls. These physiologic changes correlated with changes in the molecular machinery that produce hepatic lipids, as the mRNA expression of SREBP-1c (*Srebf1c*) and fatty-acid synthase (*Fasn*) were significantly decreased in L-p85DKO mice (Figure 5D). Interestingly, L-αKOβH mice also showed a statistically significant decrease in *Srebf1c* expression, whereas the other genotypes did not exhibit changes in either of these regulators of lipid metabolism. Since Akt activity was not diminished in these mice, we wondered if other PIP_3-dependent kinases, such as PKCλ/ζ, could be responsible for regulating the expression of *Srebf1c*.

Given the prominent role that PKCλ/ζ may play in regulating mRNA levels of SREBP-1c (Matsumoto et al., 2003), we measured PKCλ/ζ kinase activity and found that insulin normally activated PKCλ/ζ in FLOX, βKO, and L-αKO mice (Figure 5E), whereas both L-αKOβH mice and L-p85DKO mice exhibited significant defects in PKCλ/ζ activation, where insulin only marginally activated the kinase above basal levels. The magnitude of PKCλ/ζ activity paralleled the levels of *Srebf1c* expression, as has been noted in other studies (Matsumoto et al., 2003; Standaert et al., 2004).

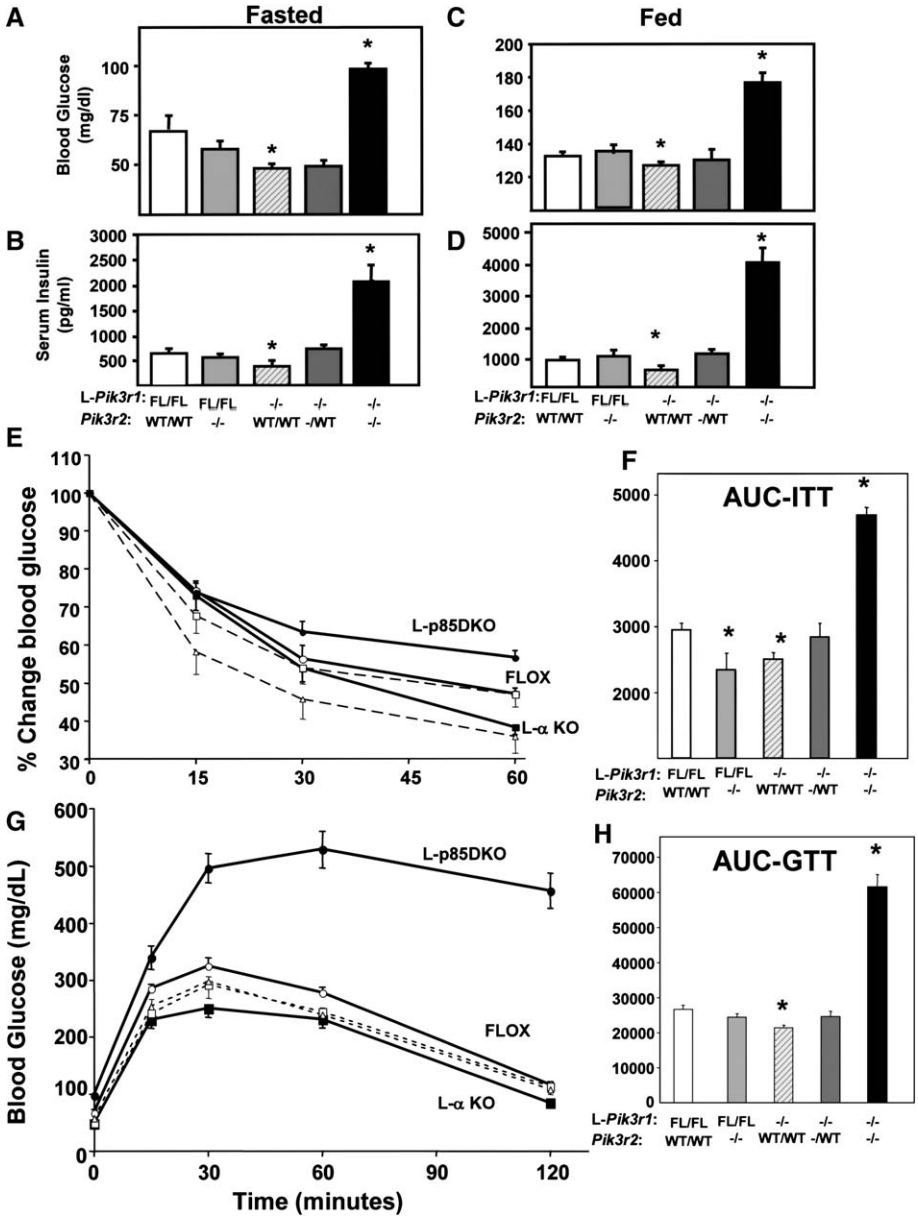

Figure 3. L-p85DKO exhibit significant defects in glucose homeostasis

Blood glucose and serum insulin levels in the fasted (**A** and **B**) and random fed (**C** and **D**) states. Glucose and insulin levels are plotted as the mean ± SEM (n = 6–12 mice per genotype).

E) Insulin tolerance tests (1 U/kg, intraperitoneally). Results represent blood glucose concentration as a percentage of starting value at zero time and are expressed as means ± SEM (n = 6–8).

F) Results from (**E**) expressed as area under ITT curves (see Experimental Procedures).

G) Glucose tolerance tests (2 g/kg, intraperitoneally) were performed on mice following a 16 hr fast. Blood samples were collected and glucose measured at the times indicated.

H) Results from (**G**) expressed as area under GTT curves (see Experimental Procedures). Bars equal ± SEM, *$p < 0.05$ compared to FLOX.

Open circles (○), bold line—FLOX; open triangles (△), dashed line—βKO; closed squares (■), bold line—L-αKO; open squares (□), dashed line—L-αKOβH; closed circles (●), bold line—L-p85DKO.

The Activation of PKCλ/ζ, but not Akt, is sufficient to upregulate hepatic SREBP-1c expression

To clarify whether Akt or PKCλ/ζ plays the dominant role in activating SREBP-1c, we reconstituted the livers of L-p85DKO mice with constitutively active forms of Akt (Myr-Akt) or PKCλ (CA-PKCλ) using adenovirus-mediated gene transfer, which specifically targets the liver (Taniguchi et al., 2005). We reasoned that the hepatic expression of constitutively active constructs in fasted L-p85DKO mice would greatly reduce the possibility of surreptitious activation of SREBP-1c by mechanisms unrelated to Akt or PKCλ/ζ. Littermate FLOX and βKO mice were also injected with these adenoviruses as genetic controls.

We first verified that we achieved the proper expression of these constructs in the liver by Western blot and kinase assay. Both constitutively active gene products are distinguishable by Western since the myr-Akt construct contains a C-terminal myc-tag (Sakoda et al., 2003) while the constitutively active PKCλ construct lacks its autoinhibitory pseudosubstrate domain and is thus truncated by approximately 15 kDa compared to wt PKCλ (Kotani et al., 1998). Immunoblots for Akt and PKCλ demonstrated that the tail vein injections successfully expressed the constitutively active constructs in the liver (Figure 6A). These constructs also increased the relative activity of each kinase, where the injection of Myr-Akt adenovirus caused a 6.0- to 8.5-fold increase in total Akt activity (Figure 6B), and the CA-PKCλ virus resulted in a 3.0- to 4.0-fold increase in PKCλ activity compared to fasted FLOX mice treated with control LacZ adenovirus (Figure 6C).

As expected, introduction of the Myr-Akt adenovirus to either the FLOX, βKO, or L-p85DKO mice resulted in the profound inhibition of both *Pck1* and *G6pc* expression in liver in all genotypes, compared to the fasted FLOX control treated with LacZ (Figures 6D and 6E). Interestingly, expression of CA-PKCλ also inhibited the expression of *Pck1* by 65%–75% and *G6Pc* by 50%–60% in all genotypes (Figures 6D and 6E), though only the *Pck1* expression was significantly different from fasted FLOX controls treated with LacZ.

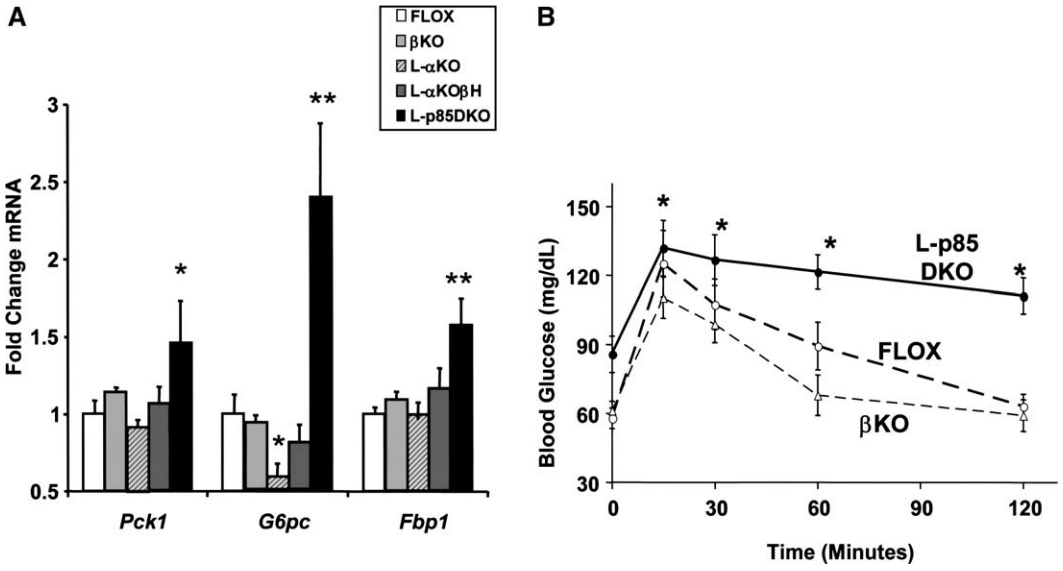

Figure 4. Defects in glucose homeostasis are linked to increased gluconeogenesis

A) Quantitative RT-PCR analysis of mRNA levels of phosphoenolpyruvate carboxykinase (*Pck1*), glucose-6-phosphatase (*G6Pc*), and fructose-1,6-bisphosphatase (*Fbp1*) in mice of the indicated genotypes.

B) Pyruvate challenge of L-p85DKO and control FLOX and βKO mice. Following a 16 hr fast, mice were injected intraperitoneally with a 2 g/kg bolus of pyruvate in normal saline. Blood glucose was then measured at the indicated time points. Open circles (○), bold dashed line—FLOX; open triangles (△), dashed line—βKO; closed circles (•), bold line—L-p85DKO. (Bars equal ± SEM, *p < 0.05, **p < 0.01 compared to FLOX.)

The expression of SREBP-1c mRNA, on the other hand, was increased by 5- to 6-fold in all genotypes by CA-PKCλ, demonstrating that atypical PKC activity is sufficient to increase *Srebf1c* levels (Figure 6F). Constitutive Akt activity, on the other hand, had no discernable effect on fasting *Srebf1c* expression as compared to mice treated with LacZ. These data demonstrate

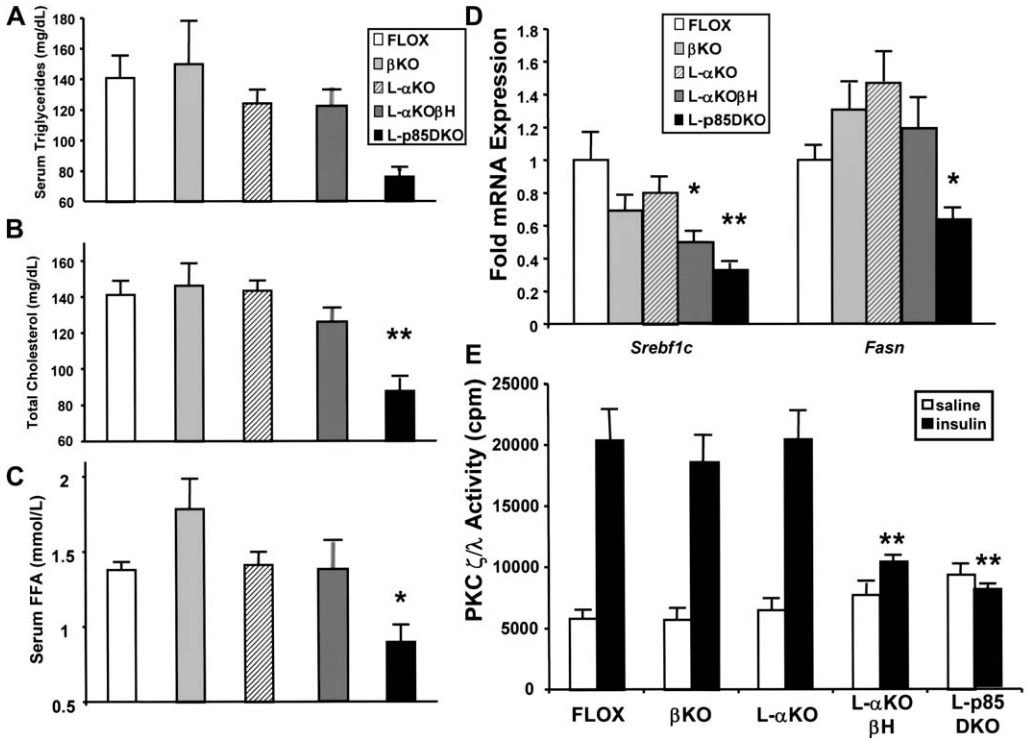

Figure 5. L-p85DKO mice are hypolipidemic

A) Serum triglycerides (**B**) cholesterol and (**C**) free fatty acids in mice of the indicated genotype (n = 6–8 ± SEM, *p < 0.05).

D) Quantitative RT-PCR analysis of mRNA levels of SREBP-1c (*Srebf1c*) and fatty-acid synthase (*Fasn*) in mice of the indicated genotypes (n = 6–8 ± SEM *p < 0.05, **p < 0.01, compared to FLOX).

E) Kinase activity of atypical protein kinase C (PKC ζ/λ) expressed as cpm. (n = 3–4 ± SEM, **p < 0.01, compared to FLOX + insulin.)

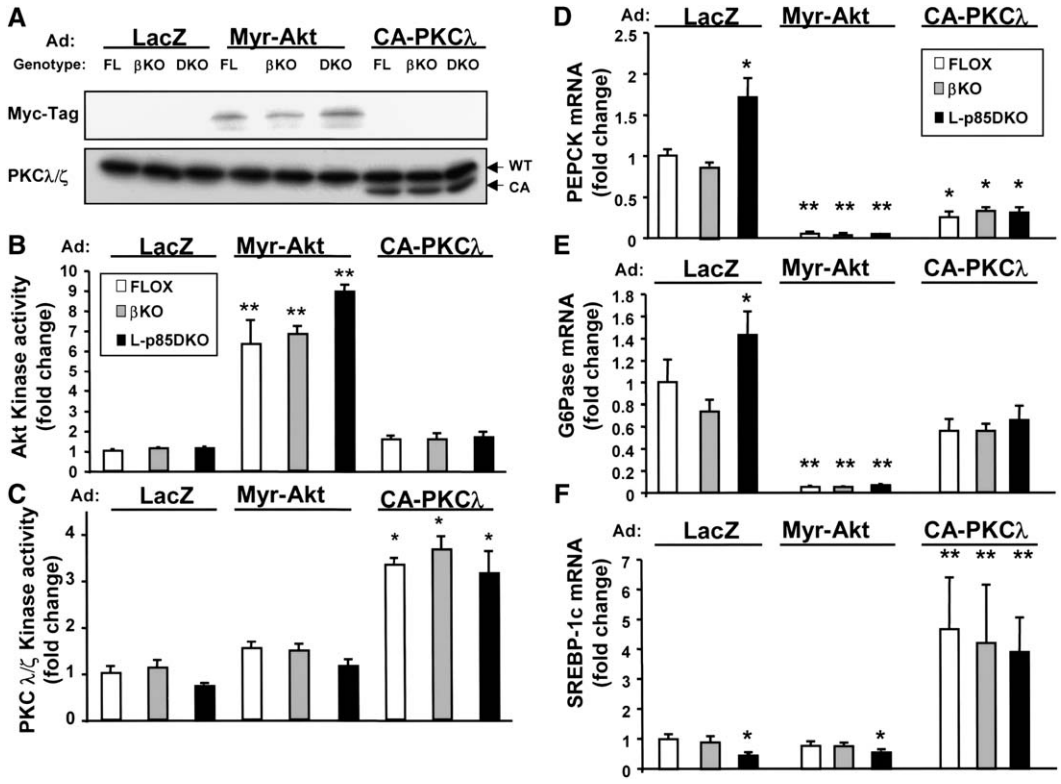

Figure 6. PKCλ/ζ activity is sufficient to increase levels of hepatic *Srebf1c* expression

A) Western blots against myc-tagged myristoylated Akt and total PKCλ/ζ in liver lysates of mice injected with the indicated adenovirus. The CA-PKCλ construct runs approximately 15 kDa smaller than wt PKCλ because it lacks the autoinhibitory pseudosubstrate domain (~115 amino acids).
B) Akt kinase activity and (**C**) PKCλ/ζ kinase activity from liver lysates of fasted mice of indicated genotype and injected with the indicated adenovirus. Quantitative RT-PCR analysis of (**D**) *Pck1*, (**E**) *G6Pc*, and (**F**) *Srebf1c* of fasted mice of indicated genotype, injected with the indicated adenovirus. The error bars represent ± SEM (n = 6–8, *p < 0.05, **p < 0.001, compared to FLOX + LacZ).

that the activity of PKCλ/ζ mediated via the PI3K pathway, and not the activity of Akt, defines the level of insulin effect on SREBP-1c expression.

Loss of hepatic PI3K causes altered liver growth and compensatory changes in body fat

The PI3K/Akt axis mediates cell growth and protein synthesis through its activation of the mTOR in a pathway involving TSC2 and p70S6 kinase. Since L-p85DKO mice exhibit significant defects in TSC2 phosphorylation and mTOR activation (Figure 2), we posited that L-p85DKO mice may also have defects in hepatocyte growth. Indeed, the livers of L-p85DKO mice were ~40% smaller than the livers of wt mice (Figure 7A). Histological examination of these livers revealed a significant increase in the number of pyknotic cells and scattered lymphocytic infiltrates in four of the five livers analyzed (Figure 7B). The livers of other genotypes were largely normal, though a small percentage of mice lacking *Pik3r1* in liver exhibited a mild degree of hepatic necrosis, as reported earlier (Fruman et al., 2000). Livers lacking all PI3K regulatory subunits were also remarkable for the presence of megahepatocytes that ranged between 40 and 60 microns in diameter as compared to an average normal hepatocyte size of between 15 and 24 microns (Figure 7B). These megahepatocytes were notable for large nuclei with cytoplasmic inclusions, indicating that these cells were likely polyploid with highly abnormal cellular function. Whether these megahepatocytes are formed from abnormal hepatocyte growth or are a product of cell fusion mediated by inflammation is unknown.

This abnormal liver histology correlated with increased levels of the hepatic enzymes, aspartate aminotransferase (AST) and alanine aminotransferase (ALT), and decreased levels of albumin in the serum of L-p85DKO (Table S1). In addition, total bilirubin levels were significantly elevated with no detectable level of direct bilirubin indicating a rise in indirect, or unconjugated, bilirubin. The presence of decreased albumin, increased AST, ALT, indirect bilirubin, and pyknotic cells in the histological samples in L-p85DKO mice is consistent with some destruction of hepatocytes and altered hepatic function (Figure 7B). The other genotypes did not display a significant increase in serum levels of AST, ALT, or bilirubin; a significant decrease in albumin; or any histological changes.

We were somewhat surprised to find that the smaller livers in L-p85DKO mice did not translate to lower overall body weights, as there were no significant weight differences between genotypes, except for a slight increase in total body weight in βKO mice (Figure 7C). We weighed other tissues in the body to determine if the weight of any one particular tissue could account for this difference, of if the normalized weight was due to a general enlargement of other tissues to maintain body weight. Surprisingly, the epididymal fat pads of the L-p85DKO mice were 2-fold heavier than the epididymal fat pads of control FLOX

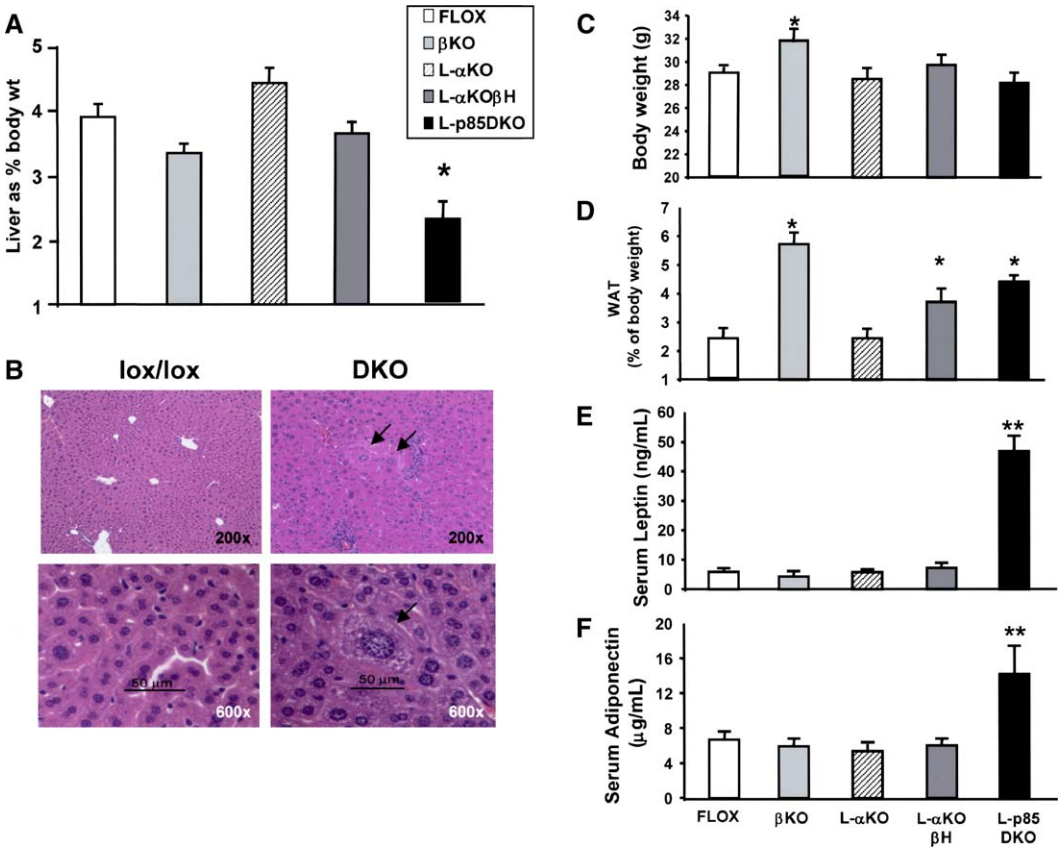

Figure 7. Lack of hepatic PI3K activity results in altered liver morphology and adipose tissue size and function

A) Liver weights from mice of the indicated genotype, normalized to total body weight.

B) Histology of L-p85DKO livers compared to control livers. Note the presence of megahepatocytes (bottom right panel) that are scattered in clusters throughout the field in L-p85DKO livers (indicated by arrows in upper right panel).

C) Total body weight and (**D**) epididymal fat pad weights of mice of the indicated genotypes.

E) Serum leptin and (**F**) serum adiponectin of various knockout mice. The bars represent ± SEM (n = 6–8, *p < 0.05, **p < 0.01, compared to FLOX).

mice, while the epididymal fat pads of βKO mice were almost 3-fold larger than controls, and the epididymal fat pads of L-αKOβH mice were ~1.8-fold greater than controls (Figure 7D).

This increase in adipose mass was accompanied by an 8-fold increase in serum leptin levels (Figure 7E) and a 2.5-fold increase in adiponectin levels (Figure 5F) in L-p85DKO mice. There was no change in these circulating adipokines in other genotypes.

Discussion

Insulin is a powerful anabolic hormone whose function in liver is to suppress gluconeogenesis and activate lipogenesis during times of nutrient excess. Thus, the loss of ablation of insulin action in liver would be predicted to cause unfettered gluconeogenesis, decreased lipogenesis, and diabetes, which is the phenotype observed in L-p85DKO mice. Interestingly, the metabolic defects of L-p85DKO mice are similar to the severe glucose intolerance and hypolipidemia observed in liver insulin receptor knockout (LIRKO) mice, further demonstrating that PI3K mediates most of insulin's regulatory functions in the liver (Michael et al., 2000).

While the prominence of the PI3K pathway in hepatic insulin action has been posited for some time, the molecular mediators of insulin's effect on glucose and lipid metabolism have only recently been explored. Our data agree with several other reports that hepatic glucose metabolism is regulated strongly by PI3K/Akt (Puigserver et al., 2003; Zhang et al., 2002). The loss of PI3K/Akt in the L-p85DKO mice impairs Akt activation by 90% and results in the increased expression of the gluconeogenic genes *Pck1*, *G6Pc*, and *Fbp1*. Conversely, the introduction of a constitutively active Akt into the livers of L-p85DKO or control animals causes >90% reduction of fasting levels of *Pck1* and *G6pc*. We also found that this regulation of gluconeogenesis was not dependent on differences in activity between Akt1 or Akt2. While we cannot rule out the possibility that the various Akt isoforms may interact with different downstream mediators or have different subcellular localization, our data suggest that it is unlikely that the differences in the biology of the Akt isoforms comes from the upstream activation by PI3K since both Akt1 and Akt2 maintained full activation until PIP_3 was fully depleted in the L-p85DKO mice.

While Akt has been clearly demonstrated to mediate insulin's suppression of gluconeogenesis, the role of Akt in the regulation of insulin-mediated lipogenesis is more controversial. Our data indicate that Akt may play only a minor role in activating lipogenesis, as the administration of a constitutively active Akt adenovirus to L-p85DKO or control animals failed to increase *Srebpf1c* levels in fasted animals. On the other hand, we demonstrated

that atypical PKC activity alone is sufficient to increase the expression of *Srebf1c* since the expression of a constitutively active PKCλ/ζ construct specifically in the hepatocytes of L-p85DKO or control animals upregulated *Srebf1c* expression 5- to 6-fold over fasted control animals injected with LacZ adenovirus. The converse relation may also be true since L-αKOβH and L-p85DKO both exhibited significant impairments in both PKCλ/ζ activity and *Srebf1c* expression. These data complement and significantly expand upon previously published knockout studies that demonstrate that atypical PKC activity is necessary for insulin-induced *Srebf1c* expression (Matsumoto et al., 2003). Together, these data suggest a primary role of PI3K/atypical PKCs in regulating *Srebf1c* levels in response to insulin.

The precise mechanisms by which PKCλ/ζ increases the transcription of SREBP-1c are not well understood. The liver X receptor (LXR) pathway has been postulated to play a primary role in the insulin-mediated induction of *Srebf1c* message levels (Chen et al., 2004). Whether the atypical PKCs interact with any factor related to the LXR pathway is not known, however, since the in vivo substrates of the atypical PKCs have not yet been defined. Indeed, the elucidation of the targets of PKCλ/ζ will be essential to understanding the molecular basis of aPKC-dependent regulation of SREBP-1c transciption.

Interestingly, the divergence in insulin's regulation of hepatic glucose and lipid was detected due to a difference in the activation of Akt and aPKC in the various p85 hypomorphs. Our data suggest that Akt may be more sensitive to insulin/PIP_3 than PKCλ/ζ since Akt could be fully activated in the αKOβHet mice despite the fact the levels of PIP_3 were reduced by ~50% (see Figure 1D), while PKCλ/ζ activity in these mice was markedly diminished (see Figure 5E). The molecular basis for this differential activation is not known but could be due to differences in their PIP_3 binding or some other aspect of aPKC activation, such as autophosphorylation or inhibition by its pseudosubstrate domain (Farese et al., 2005).

Phosphoinositide 3-kinase controls several other important aspects of hepatocyte function in addition to metabolism. In particular, the PI3K/Akt/mTOR pathway was severely impaired in L-p85DKO mice as manifested by decreased TSC2 and S6 phosphorylation. These defects in translational control by PI3K lead to a 40% decrease in liver size and a 60% decrease in albumin synthesis. In addition, L-p85DKO mice exhibited abnormal histology and elevated levels of serum AST, ALT, and indirect (unconjugated) bilirubin (see Table S1). Despite these indications of liver damage, L-p85DKO mice were able to respond in an exaggerated way to a pyruvate challenge (Figure 4B), indicating that the hyperglycemia and probably the other defects in glucose homeostasis in L-p85DKO mice were a result of the increased expression of functional gluconeogenic enzymes (Figure 4A), and not some aspect of hepatic insufficiency.

The loss of hepatic PI3K activity also led to changes in adipose tissue physiology. The epididymal fat pads in the L-p85DKO were almost 2-fold larger than controls, which is most likely due to the moderate and persistent hyperinsulinemia that leads to a substrate shift to adipocytes. This phenomenon has been observed in other models of insulin resistance and diabetes such as liver insulin receptor knockout (LIRKO) mice (Michael et al., 2000) and muscle insulin receptor knockout (MIRKO) mice (Bruning et al., 1998). In addition, L-p85DKO mice exhibited significant increases in the two major adipokines, leptin and adiponectin. These increases are probably not a cell-autonomous effect of adipose tissue since the elevated leptin and adiponectin are increased only in the L-p85DKO mice, despite the βKO and L-αKOβH mice having epididymal fat pads nearly equal in size or larger than those in the L-p85DKO mice. Interestingly, LIRKO mice also display striking increases in serum leptin levels (>60-fold over controls) as a compensatory response to a 450-fold increase in soluble leptin receptor expression by the liver (Cohen and C.R.K., unpublished data). The relationship between insulin-stimulated PI3K activity and leptin receptor expression observed in LIRKO may also explain the elevated leptin levels in L-p85DKO mice, as L-p85DKO mice have a 12-fold increase in soluble leptin receptor expression (data not shown) to match the 5-fold increase in serum leptin (Figure 7E).

In summary, deletion of all major regulatory subunits of PI3K in liver results in a marked reduction in insulin-stimulated PI3K activity and PIP_3 accumulation in liver and significant defects in glucose and lipid homeostasis, as well as in hepatic size and function. Thus, the PI3K pathway is essential for metabolic homeostasis and cell growth, and PI3K activity is responsible for nearly all of insulin's actions in the liver in vivo. Moreover, the specific regulation of glucose and lipid homeostasis by insulin diverges after PI3K activation, where it appears that Akt selectively and potently regulates gluconeogenesis whereas PKCλ/ζ increases *Srebf1c* expression. The differential actions of the PI3K-dependent kinases, Akt and PKCλ/ζ, may represent the primary mechanisms by which insulin regulates different aspects of hepatic metabolism. Understanding these mechanisms not only helps to clarify the important regulators in hepatic function but may also provide more specific ways to improve many complications of diabetes and the metabolic syndrome.

Experimental procedures

Animals and breeding strategy

All animals were housed on a 12 hr light-dark cycle and fed a standard rodent chow. All protocols for animal use and euthanasia were approved by the Animal Care Use Committee of the Joslin Diabetes Center and Harvard Medical School in accordance with National Institutes of Health guidelines. All mice in this study were on a 129Sv-C57BL/6-FVB mixed genetic background. The breeding strategy in this study involved the crossing of homozygous floxed *Pik3r1* mice with *Pik3r2* homozygous null mice to create mice homozygous for both the *Pik3r1* floxed allele and the *Pik3r2* null allele (*Pik3r1*$^{fl/fl}$, *Pik3r2*$^{-/-}$). These mice were then bred with L-αKOβH (L-*Pik3r1*$^{-/-}$, *Pik3r2*$^{+/-}$) mice, also on a mixed background, which contain the albumin-Cre transgene, to produce the five groups used in this study.

Quantitative Reverse Transcription PCR analysis

Total RNA was isolated from mouse tissues using an RNeasy kit (QIAGEN, Valencia, California). cDNA was prepared from 1 μg of RNA using the Advantage RT-PCR kit (BD Biosciences, Palo Alto, California) with random hexamer primers, according to manufacturer's instructions. The resulting cDNA was diluted 10-fold, and a 5 μl aliquot was used in a 20 μl PCR reaction (SYBR Green, PE Biosystems) containing primers at a concentration of 300 nM each. PCR reactions were run in triplicate and quantitated in the ABI Prism 7700 Sequence Detection System. Ct values were normalized to TATA box binding protein (TBP) expression, and results were expressed as a fold change of mRNA compared to the indicated control mice. Primers for *Pck1*, *G6Pc*, *Fbp1*, *Srebf1c*, and *Fasn* were described previously (Taniguchi et al., 2005). Primers for p85β were designed across exon 1 and exon 2 since exon 1 is deleted in *Pik3r2* knockout mice. The forward primer for p85β is CCCTTGGATG GATCTTCTGA and the reverse primer is TCCACCAGCTTCACCAGAAT.

Metabolic studies

For glucose tolerance testing (GTT), blood samples were obtained at 0, 15, 30, 60, and 120 min after intraperitoneal injection of 2 g/kg dextrose. Insulin

tolerance tests were performed by injecting 1 U/kg insulin (Novolin, Novo Nordisk, Denmark) intraperitoneally, followed by blood collection at 0, 15, 30, and 60 min. The pyruvate challenge was performed by injected 2 g/kg of pyruvate (Sigma) intraperitoneally, with blood glucose measured at 0, 15, 30, and 60 min time points. Blood glucose values were determined using a One Touch II glucose monitor (Lifescan Inc., Milipitas, California). Serum insulin and leptin levels were measured by ELISA using mouse insulin as a standard (Crystal Chem Inc., Chicago, Illinois). Serum adiponectin levels were analyzed from diluted mouse serum (1/1000) and analyzed by an ELISA kit (Linco). Nonesterified free fatty-acid levels were measured from random fed mice using a kit from Wako Diagnostics. The serum levels of the liver enzymes, bilirubin, total protein albumin, and triglycerides were measured by Anilytics (Gaithersburg, Maryland).

In vivo insulin signaling

Following an overnight fast, mice were anesthetized with 2,2,2-tribromoethanol in PBS (Avertin), and injected with 5 U of regular human insulin (Novolin, Novo Nordisk, Denmark) via the inferior vena cava. Five minutes after the insulin bolus, tissues were removed and frozen in liquid nitrogen. Immunoprecipitation and immunoblot analysis of insulin signaling molecules were performed using tissue homogenates prepared in a tissue homogenization buffer that contained 25 mM Tris-HCl (pH 7.4), 10 mM Na_3VO_4, 100 mM NaF, 50 mM $Na_4P_2O_7$, 10 mM EGTA, 10 mM EDTA, 2 mM phenylmethylsulfonyl fluoride, 1% Nonidet-P40 supplemented with the Complete protease inhibitor cocktail (Roche). All protein expression data were quantified by densitometry using NIH Image.

Antibodies

Rabbit polyclonal anti-IRS-1 antibody (IRS-1), anti-IRS-2 antibody (IRS-2), anti-IR antibody (IR), and pan-p85α antibody were generated as described previously (Ueki et al., 2002). Rabbit polyclonal anti-Akt, anti-phospho Akt (S473), anti-phospho FoxO1, anti-phospho GSK3β (Ser9), anti-FoxO1, anti-GSK3, anti-phosphoTSC2 (Thr1462), anti-TSC2, anti-phospho S6 (Ser240/244), and anti-S6 antibodies were purchased from Cell Signaling Technology (Beverly, Massachusetts). Myc-tag and isoform-specific Akt antibodies were purchased from Upstate Biotechnology (Lake Placid, New York). A polyclonal antibody for Westerns and immunoprecipitation against PKCλ/ζ was purchased from Santa Cruz Biotechnology.

PIP_3 quantitation

Phosphatidylinositol(3,4,5)-triphosphate (PIP_3) levels were measured by a monoclonal antibody (IgM, Echelon Biosciences) as described previously (Kitamura et al., 2004), with a few modifications. Following insulin or saline treatment, mice were fixed by cardiac perfusion of 10% buffered formalin. The livers were then dehydrated in 30% sucrose overnight, then frozen in OCT compound (Sakura) for sectioning. For quantification of the immunofluorescence, four representative slides were chosen from each mouse and the fluorescence intensity of 16 fields per slide was measured and analyzed with VH-H1A5 analyzer software (KEYENCE, Osaka, Japan).

In vitro kinase assays

Livers were extracted into tissue homogenization buffer and subjected to immunoprecipitation with IRS-1, IRS-2, or pTyr for PI3K assays as described previously (Taniguchi et al., 2005). Isoform-specific Akt antibodies were used to immunoprecipitate Akt1 or Akt2 from liver lysates then were subjected to Crosstide assay as described previously (Sakamoto et al., 2002). Reactions for atypical PKC activity were performed as reported previously (Sajan et al., 2004).

Statistics

Data are presented as ± SEM. Student's t test was used for statistical analysis between two groups, while statistical significance between multiple treatment groups was determined by analysis of variance (ANOVA) and Tukey's t test. The trapezoid method was used to calculate area under the curve for ITT and GTT curves (Tran et al., 1996).

Supplemental data

Supplemental data include one table and can be found with the article online at http://www.cellmetabolism.org/cgi/content/full/3/5/343/DC1/.

Acknowledgments

We greatly appreciate the technical assistance of Laureen Mazzola and Will Wisdom. This work was supported by National Institutes of Health Grants DK33201 and DK55545, Joslin Diabetes and Endocrinology Research Center Grant DK34834 (to C.R.K.), and a GM41890 and CA089021 for L.C.C. C.M.T. acknowledges support from the American Diabetes Association Medical Scholars Award (C.M.T.) and a Medical Scientist Training Program scholarship (Harvard Medical School). J.L. acknowledges support from a HHMI predoctoral fellowship.

Received: December 22, 2005
Revised: March 22, 2006
Accepted: April 14, 2006
Published: May 9, 2006

References

Bi, L., Okabe, I., Bernard, D.J., Wynshaw-Boris, A., and Nussbaum, R.L. (1999). Proliferative defect and embryonic lethality in mice homozygous for a deletion in the p110alpha subunit of phosphoinositide 3-kinase. J. Biol. Chem. *274*, 10963–10968.

Bi, L., Okabe, I., Bernard, D.J., and Nussbaum, R.L. (2002). Early embryonic lethality in mice deficient in the p110beta catalytic subunit of PI 3-kinase. Mamm. Genome *13*, 169–172.

Bruning, J.C., Michael, M.D., Winnay, J.N., Hayashi, T., Horsch, D., Accili, D., Goodyear, L.J., and Kahn, C.R. (1998). A muscle-specific insulin receptor knockout exhibits features of the metabolic syndrome of NIDDM without altering glucose tolerance. Mol. Cell *2*, 559–569.

Chen, G., Liang, G., Ou, J., Goldstein, J.L., and Brown, M.S. (2004). Central role for liver X receptor in insulin-mediated activation of Srebp-1c transcription and stimulation of fatty acid synthesis in liver. Proc. Natl. Acad. Sci. USA *101*, 11245–11250.

Cho, H., Mu, J., Kim, J.K., Thorvaldsen, J.L., Chu, Q., Crenshaw, E.B., 3rd, Kaestner, K.H., Bartolomei, M.S., Shulman, G.I., and Birnbaum, M.J. (2001). Insulin resistance and a diabetes mellitus-like syndrome in mice lacking the protein kinase Akt2 (PKB beta). Science *292*, 1728–1731.

Cross, D.A., Alessi, D.R., Cohen, P., Andjelkovich, M., and Hemmings, B.A. (1995). Inhibition of glycogen synthase kinase-3 by insulin mediated by protein kinase B. Nature *378*, 785–789.

Farese, R.V., Sajan, M.P., and Standaert, M.L. (2005). Atypical protein kinase C in insulin action and insulin resistance. Biochem. Soc. Trans. *33*, 350–353.

Fleischmann, M., and Iynedjian, P.B. (2000). Regulation of sterol regulatory-element binding protein 1 gene expression in liver: role of insulin and protein kinase B/cAkt. Biochem. J. *349*, 13–17.

Fruman, D.A., Mauvais-Jarvis, F., Pollard, D.A., Yballe, C.M., Brazil, D., Bronson, R.T., Kahn, C.R., and Cantley, L.C. (2000). Hypoglycaemia, liver necrosis and perinatal death in mice lacking all isoforms of phosphoinositide 3-kinase p85 alpha. Nat. Genet. *26*, 379–382.

Harris, T.E., and Lawrence, J.C., Jr. (2003). TOR signaling. Sci. STKE *2003*, re15.

Jiang, Z.Y., Zhou, Q.L., Coleman, K.A., Chouinard, M., Boese, Q., and Czech, M.P. (2003). Insulin signaling through Akt/protein kinase B analyzed by small interfering RNA-mediated gene silencing. Proc. Natl. Acad. Sci. USA *100*, 7569–7574.

Kitamura, T., Kitamura, Y., Nakae, J., Giordano, A., Cinti, S., Kahn, C.R., Efstratiadis, A., and Accili, D. (2004). Mosaic analysis of insulin receptor function. J. Clin. Invest. *113*, 209–219.

Kotani, K., Ogawa, W., Matsumoto, M., Kitamura, T., Sakaue, H., Hino, Y., Miyake, K., Sano, W., Akimoto, K., Ohno, S., and Kasuga, M. (1998). Requirement of atypical protein kinase clambda for insulin stimulation of glucose uptake but not for Akt activation in 3T3–L1 adipocytes. Mol. Cell. Biol. *18*, 6971–6982.

Luo, J., McMullen, J.R., Sobkiw, C.L., Zhang, L., Dorfman, A.L., Sherwood, M.C., Logsdon, M.N., Horner, J.W., Depinho, R.A., Izumo, S., and Cantley, L.C. (2005). Class IA phosphoinositide 3-kinase regulates heart size and physiological cardiac hypertrophy. Mol. Cell. Biol. *25*, 491–502.

Matsumoto, M., Ogawa, W., Akimoto, K., Inoue, H., Miyake, K., Furukawa, K., Hayashi, Y., Iguchi, H., Matsuki, Y., Hiramatsu, R., et al. (2003). PKClambda in liver mediates insulin-induced SREBP-1c expression and determines both hepatic lipid content and overall insulin sensitivity. J. Clin. Invest. *112*, 935–944.

Michael, M.D., Kulkarni, R.N., Postic, C., Previs, S.F., Shulman, G.I., Magnuson, M.A., and Kahn, C.R. (2000). Loss of insulin signaling in hepatocytes leads to severe insulin resistance and progressive hepatic dysfunction. Mol. Cell *6*, 87–97.

Ono, H., Shimano, H., Katagiri, H., Yahagi, N., Sakoda, H., Onishi, Y., Anai, M., Ogihara, T., Fujishiro, M., Viana, A.Y., et al. (2003). Hepatic Akt activation induces marked hypoglycemia, hepatomegaly, and hypertriglyceridemia with sterol regulatory element binding protein involvement. Diabetes *52*, 2905–2913.

Postic, C., and Magnuson, M.A. (2000). DNA excision in liver by an albumin-Cre transgene occurs progressively with age. Genesis *26*, 149–150.

Potter, C.J., Pedraza, L.G., and Xu, T. (2002). Akt regulates growth by directly phosphorylating Tsc2. Nat. Cell Biol. *4*, 658–665.

Puigserver, P., Rhee, J., Donovan, J., Walkey, C.J., Yoon, J.C., Oriente, F., Kitamura, Y., Altomonte, J., Dong, H., Accili, D., and Spiegelman, B.M. (2003). Insulin-regulated hepatic gluconeogenesis through FOXO1-PGC-1alpha interaction. Nature *423*, 550–555.

Sajan, M.P., Standaert, M.L., Miura, A., Kahn, C.R., and Farese, R.V. (2004). Tissue-specific differences in activation of atypical protein kinase C and protein kinase B in muscle, liver, and adipocytes of insulin receptor substrate-1 knockout mice. Mol. Endocrinol. *18*, 2513–2521.

Sakamoto, K., Hirshman, M.F., Aschenbach, W.G., and Goodyear, L.J. (2002). Contraction regulation of Akt in rat skeletal muscle. J. Biol. Chem. *277*, 11910–11917.

Sakoda, H., Gotoh, Y., Katagiri, H., Kurokawa, M., Ono, H., Onishi, Y., Anai, M., Ogihara, T., Fujishiro, M., Fukushima, Y., et al. (2003). Differing roles of Akt and serum- and glucocorticoid-regulated kinase in glucose metabolism, DNA synthesis, and oncogenic activity. J. Biol. Chem. *278*, 25802–25807.

Shepherd, P.R., Withers, D.J., and Siddle, K. (1998). Phosphoinositide 3-kinase: the key switch mechanism in insulin signalling. Biochem. J. *333*, 471–490.

Shimomura, I., Bashmakov, Y., Ikemoto, S., Horton, J.D., Brown, M.S., and Goldstein, J.L. (1999). Insulin selectively increases SREBP-1c mRNA in the livers of rats with streptozotocin-induced diabetes. Proc. Natl. Acad. Sci. USA *96*, 13656–13661.

Standaert, M.L., Sajan, M.P., Miura, A., Kanoh, Y., Chen, H.C., Farese, R.V., Jr., and Farese, R.V. (2004). Insulin-induced activation of atypical protein kinase C, but not protein kinase B, is maintained in diabetic (ob/ob and Goto-Kakazaki) liver. Contrasting insulin signaling patterns in liver versus muscle define phenotypes of type 2 diabetic and high fat-induced insulin-resistant states. J. Biol. Chem. *279*, 24929–24934.

Taniguchi, C.M., Ueki, K., and Kahn, R. (2005). Complementary roles of IRS-1 and IRS-2 in the hepatic regulation of metabolism. J. Clin. Invest. *115*, 718–727.

Taniguchi, C.M., Emanuelli, B., and Kahn, C.R. (2006). Critical nodes in signalling pathways: insights into insulin action. Nat. Rev. Mol. Cell Biol. *7*, 85–96.

Terauchi, Y., Tsuji, Y., Satoh, S., Minoura, H., Murakami, K., Okuno, A., Inukai, K., Asano, T., Kaburagi, Y., Ueki, K., et al. (1999). Increased insulin sensitivity and hypoglycaemia in mice lacking the p85 alpha subunit of phosphoinositide 3-kinase. Nat. Genet. *21*, 230–235.

Tran, T.T., Medline, A., and Bruce, W.R. (1996). Insulin promotion of colon tumors in rats. Cancer Epidemiol. Biomarkers Prev. *5*, 1013–1015.

Ueki, K., Algenstaedt, P., Mauvais-Jarvis, F., and Kahn, C.R. (2000). Positive and negative regulation of phosphoinositide 3-kinase-dependent signaling pathways by three different gene products of the p85alpha regulatory subunit. Mol. Cell. Biol. *20*, 8035–8046.

Ueki, K., Yballe, C.M., Brachmann, S.M., Vicent, D., Watt, J.M., Kahn, C.R., and Cantley, L.C. (2002). Increased insulin sensitivity in mice lacking p85beta subunit of phosphoinositide 3-kinase. Proc. Natl. Acad. Sci. USA *99*, 419–424.

Ueki, K., Fruman, D.A., Yballe, C.M., Fassaur, M., Klein, J., Asano, T., Cantley, L.C., and Kahn, C.R. (2003). Positive and negative roles of p85alpha and p85beta regulatory subunits of phosphoinositide 3-kinase in insulin signaling. J. Biol. Chem. *278*, 48453–48466.

Zhang, X., Gan, L., Pan, H., Guo, S., He, X., Olson, S.T., Mesecar, A., Adam, S., and Unterman, T.G. (2002). Phosphorylation of serine 256 suppresses transactivation by FKHR (FOXO1) by multiple mechanisms. Direct and indirect effects on nuclear/cytoplasmic shuttling and DNA binding. J. Biol. Chem. *277*, 45276–45284.